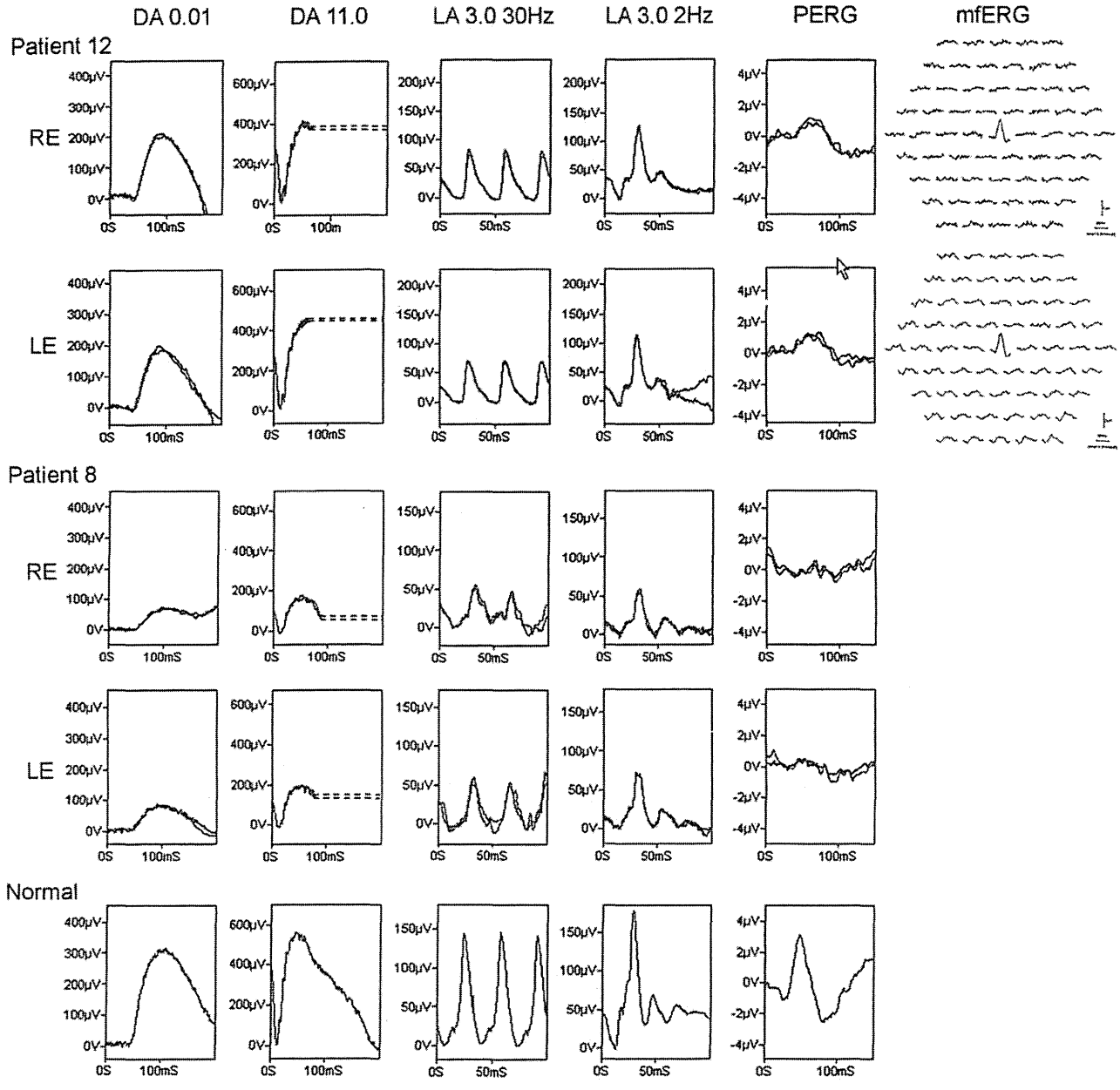

FIGURE 5. Full-field electroretinograms, pattern electroretinograms, and multifocal electroretinograms from 2 representative cases with the foveal-sparing phenotype of Stargardt disease, showing localized spared foveal function and marked macular dysfunction with generalized rod and cone system involvement, respectively (Patients 12 and 8). Full-field electroretinograms (ERGs) included: (1) dark-adapted dim flash 0.01 candela-seconds per square meter ($cd \cdot s \cdot m^{-2}$) (DA 0.01); (2) dark-adapted bright flash 11.0 $cd \cdot s \cdot m^{-2}$ (DA 11.0); (3) light-adapted 3.0 $cd \cdot s \cdot m^{-2}$ 30 Hz flicker (LA 3.0 30 Hz); and (4) light-adapted 3.0 $cd \cdot s \cdot m^{-2}$ at 2 Hz (LA 3.0 2 Hz). Patient 12 demonstrates normal ERGs and subnormal P50 components of pattern electroretinogram (PERG), consistent with macular dysfunction; multifocal electroretinograms (mfERGs) reveal sparing of localized foveal function with severe paracentral macular dysfunction bilaterally. Patient 8 has abnormal ERGs, consistent with generalized rod and cone system dysfunction, with marked PERG P50 reduction indicating marked macular involvement. Normal traces are shown for comparison.

The electrophysiological findings are summarized in Table 1; representative traces appear in Figure 5.

• MOLECULAR GENETICS: Likely disease-causing *ABCA4* variants were detected in 31 of 40 patients: 2 or more variants were identified in 16 patients and 1 variant in 15 subjects (Table 1). Detailed results, including in silico analysis to assist in the prediction of pathogenicity of the variants, are shown in Table 2. Thirty variants were found in 31 patients: 7 null variants, with 3 predicted to affect splicing

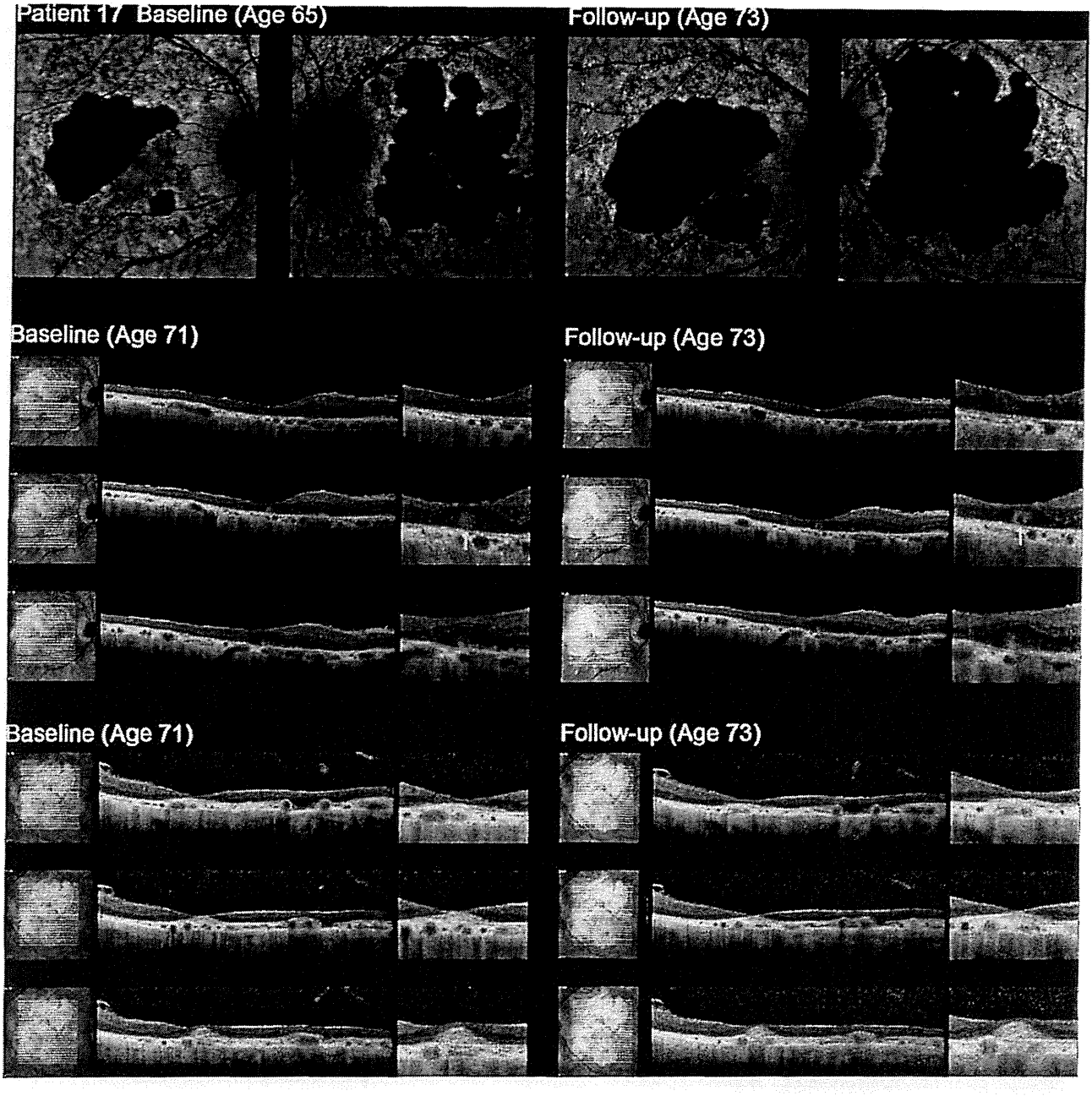

FIGURE 4. Serial autofluorescence and spectral-domain optical coherence tomographic images of Patient 17, with the foveal-sparing phenotype of Stargardt disease, illustrating enlargement of atrophy and progression of a snowball-like lesion to a recognizable outer retinal tubulation. Autofluorescence images at baseline show multiple patchy asymmetrical atrophic lesions in each eye. LogMAR visual acuity was −0.08 in the right eye but 1.0 in the left eye at baseline. Enlargement of the areas of atrophy occurs over time, with relative preservation of the foveal autofluorescence signal in the right eye (logMAR visual acuity 0.18). Disruption of outer retinal structure, with a snowball-like lesion (arrow) at the fovea in the right eye and foveal atrophy in the left eye, is present in baseline optical coherence tomographic images. The snowball-like lesion progresses over time, with outer retinal tubulation clearly present at follow-up in the right eye.

eyes of 3 patients (9%), abnormal responses in either eye of 16 subjects (48%), and undetectable responses in either eye of 14 individuals (42%). The median PERG P50 amplitude of PERG was 0.5 μV (range, 0.0-3.6 μV). The mfERG showed preservation of the response to the central hexagon surrounded by reduced responses to the paracentral hexagons in 3 of 8 patients (38%). These 3 patients had normal full-field ERGs. Five of 8 subjects (62%) had severely reduced central and paracentral responses, including 2 with normal ERGs and 3 with the group 3 ERG phenotype.

FIGURE 3. Serial autofluorescence and spectral-domain optical coherence tomographic images of Patient 9, with the foveal-sparing phenotype of Stargardt disease, showing increasing of atrophy and architectural disruption. Patient 9 presented without any visual symptoms 5 years prior to the most recent examination. LogMAR visual acuity was 0.0 in each eye. Autofluorescence images show numerous foci of high or low signal at the posterior pole at baseline, with increasing atrophy over time. Optical coherence tomographic images at baseline show relatively preserved foveal structure with an intact junction between the inner and outer photoreceptor segments (IS/OS) in each eye; IS/OS disruption is present at follow-up examination.

Fifteen patients (45%) showed evidence of outer retinal tubulation. The median age of onset and the mean duration of disease of these 15 patients with outer retinal tubulation were 45.0 and 7.2 years, compared to 43.0 and 2.1 years for the 18 subjects without outer retinal tubulation. The median visual acuity was the same in both groups. AF and SDOCT images of 2 representative cases (Patients 9 and 17) demonstrate slow progression over time (Figures 3 and 4).

Electrophysiological assessment was performed in 33 patients. ERG and PERG were recorded in all; mfERG was obtained in 8 individuals. Twenty-two of the 33 patients (67%) were in ERG group 1, 3 (9%) in ERG group 2, and 8 (24%) in ERG group 3. PERG was normal in both

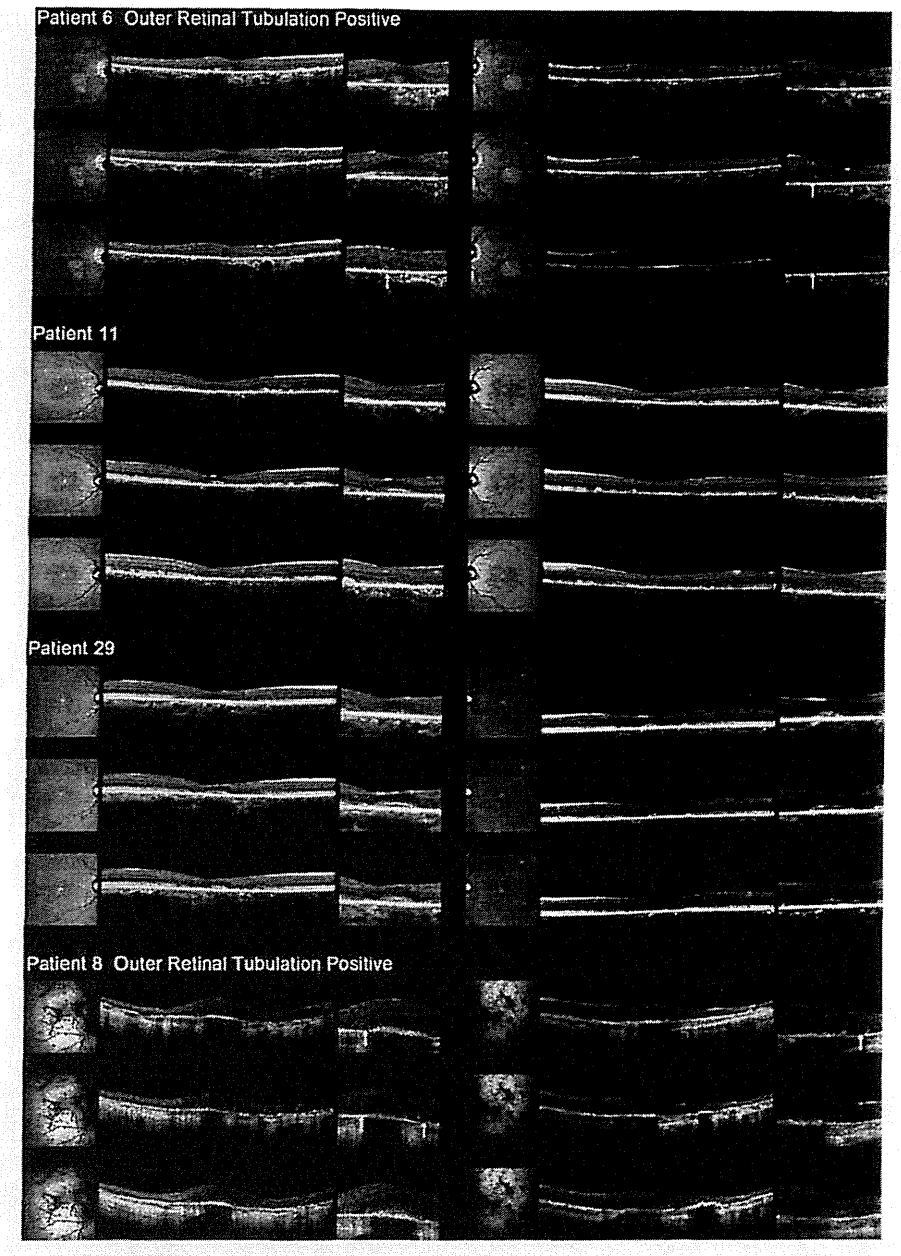

FIGURE 2. Spectral-domain optical coherence tomographic images of the 4 representative cases with the foveal-sparing phenotype of Stargardt disease illustrated in Figure 1 (Patients 6, 11, 29, and 8), demonstrating relatively preserved foveal structure and outer retinal tubulation. There is relatively preserved foveal structure in all 4 patients, with 2 showing outer retinal tubulation (Patients 6 and 8). Arrows in the magnified images identify outer retinal tubulation.

RPE changes and/or localized parafoveal yellow-white flecks; and pattern 4 (n = 2, 5%) had multiple patchy atrophic lesions, extending beyond the arcades. One patient (2.5%) had a bull's-eye maculopathy (Patient 33). These data are summarized in Table 1. The median ages of onset of patterns 1, 2, 3, and 4 were 46.0, 39.5, 36.0, and 43.5 years, respectively; the mean duration of disease was 5.1, 0.1, 2.9, and 15.0 years. The median logMAR visual acuity of patterns 1, 2, 3, and 4 was 0.18, 0.00, 0.18, and 0.05, respectively. Color fundus photographs and AF images of 4 representative cases are shown in Figure 1, with associated OCT images in Figure 2.

SDOCT images were obtained in 33 individuals (Table 1). The median central foveal thickness of the right and left eyes was 180.0 μm and 185.0 μm, respectively (range, 32-219 μm and 39-273 μm). The median central foveal thickness for each fundus pattern in the right eye was 179.5 μm for pattern 1 (18 patients); 223.5 μm for pattern 2 (6 subjects); 159.5 μm for pattern 3 (6 individuals); and 216.0 μm for pattern 4 (2 patients).

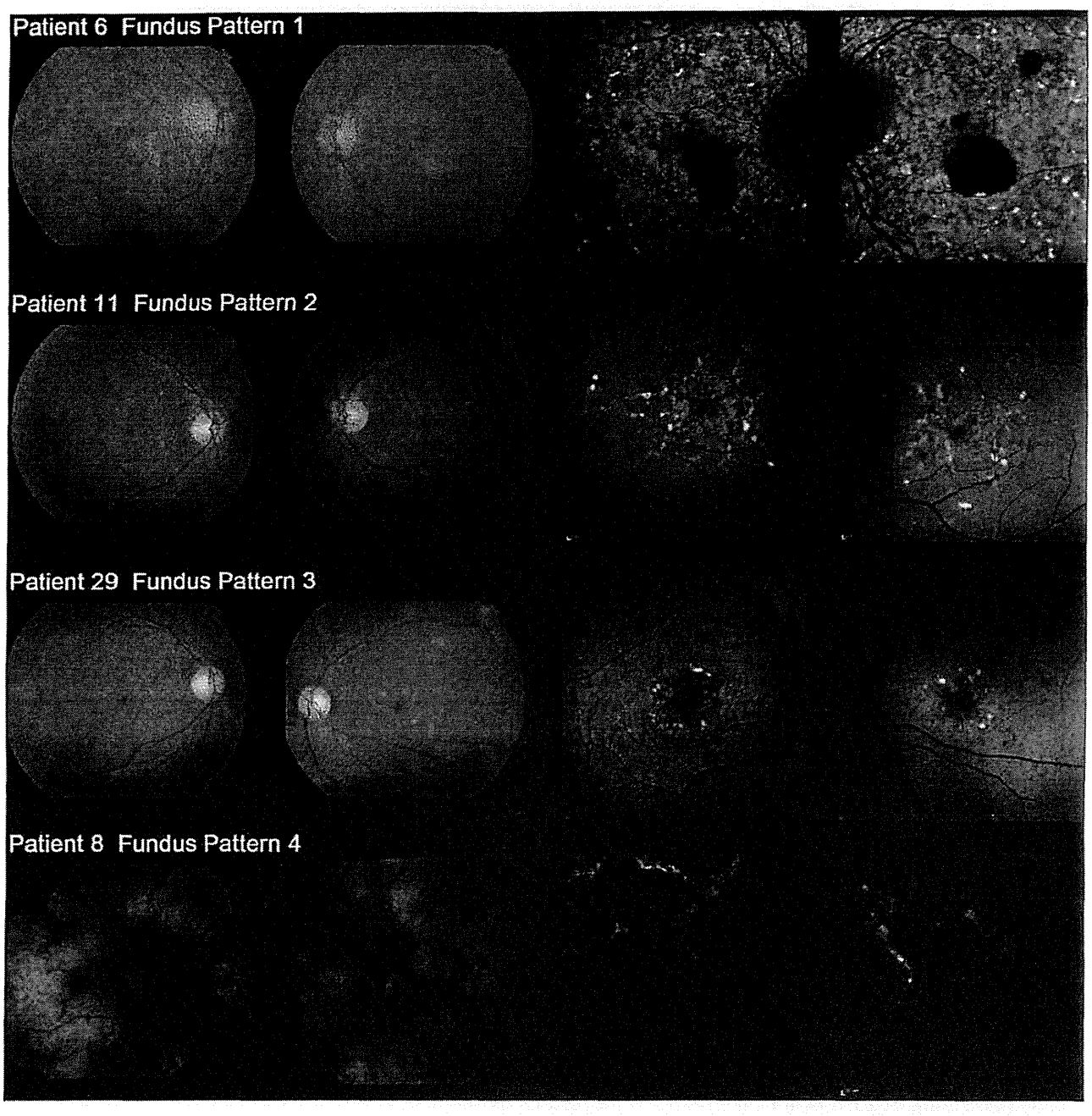

FIGURE 1. Color fundus photographs and autofluorescence images of 4 representative cases with a foveal-sparing phenotype of Stargardt disease (Patients 6, 11, 29, and 8), showing 4 fundus phenotypes identified in this study, respectively. Images show examples of each of 4 fundus phenotypes identified in this study: Patient 6 shows pattern 1 (patchy parafoveal atrophy surrounded by numerous yellow-white flecks); Patient 11 shows pattern 2 (numerous yellow-white flecks at the posterior pole without atrophy); Patient 29 shows pattern 3 (mottled retinal pigment epithelium changes and localized parafoveal yellow-white flecks); and Patient 8 shows pattern 4 (multiple patchy atrophic lesions, extending beyond the arcades).

−0.08 to 2.0 and −0.08 to 3.0). Two patients (4 and 26) had a logMAR visual acuity of less than 1.0 in the right eye at the most recent review, with those patients having been diagnosed with the foveal-sparing phenotype of Stargardt disease 4 years earlier, when visual acuity was 0.18 in the right eye and 0.48 in the left eye.

Color fundus photography was performed in all 40 patients. Four patterns were identified: pattern 1 (n = 22, 55%) showed patchy parafoveal atrophy surrounded by numerous yellow-white flecks; pattern 2 (n = 8, 20%) had numerous yellow-white flecks at the posterior pole without atrophy; pattern 3 (n = 7, 17.5%) had mottled

TABLE 1. Summary of Clinical Findings and Molecular Status of 40 Patients With a Foveal-Sparing Phenotype[a] of Stargardt Disease (*Continued*)

Patient	Onset[b] (y)	Age (y)	LogMAR Visual Acuity OD	LogMAR Visual Acuity OS	Fundus Pattern[c]	OCT CFT[d] (μm) OD	OCT CFT[d] (μm) OS	OCT ORT	ERG[e] Group	ERG[e] PERG OD	ERG[e] PERG OS	ERG[e] mfERG OD	ERG[e] mfERG OS	Mutation Status
33	39	40	0.18	0	5	126	140		NA	NA	NA	NA	NA	Not detected
34	25*	25	0.18	0	3	147	150		NA	NA	NA	NA	NA	Not detected
35	29	36	0	0.3	3	172	181		2	A	A	NA	NA	Not detected
36	40	45	0.3	0	1	NA	NA		1	A	N	NA	NA	Not detected
37	35	41	0.18	0.18	1	150	131	✓	1	ND	ND	NA	NA	Not detected
38	29*	29	−0.1	0	2	237	236		NA	NA	NA	NA	NA	Not detected
39	25	35	−0.1	0	1	237	179	✓	3	ND	ND	2	2	Not detected
40	75	75	0.18	0.18	1	194	186		NA	NA	NA	NA	NA	Not detected

A = abnormal; CFT = central foveal thickness; ERG = electroretinogram; mfERG = multifocal ERG; N = normal; NA = not available; ND = not detectable; OCT = optical coherence tomography; ORT = outer retinal tubulation; PERG = pattern ERG.

[a]The foveal-sparing phenotype was defined as foveal preservation on autofluorescence imaging, despite a retinopathy otherwise consistent with Stargardt disease.

[b]The age of onset was defined as the age at which visual loss was first noted by the patient or as the age at the latest examination for patients (labeled with*) who are not aware of any visual symptom. Two patients complained of diplopia (labeled with**).

[c]Color fundus photography identified 4 patterns: pattern 1, patchy parafoveal atrophy surrounded by numerous yellow-white flecks; pattern 2, numerous yellow-white flecks at the posterior pole without atrophy; pattern 3, mottled retinal pigment epithelial changes and/or localized parafoveal yellow-white flecks; pattern 4, multiple patchy atrophic lesions, extending beyond the arcades. One patient had a bull's-eye maculopathy appearance (Patient 33, labeled as pattern 5).

[d]The CFT was defined as the distance between inner retinal surface and inner border of retinal pigment epithelium.

[e]Patients were classified on the basis of electrophysiological findings: group 1 - normal ERGs with or without PERG P50 abnormality; group 2 - PERG P50 abnormality and additional generalized cone system abnormality; group 3 - PERG P50 abnormality and additional generalized cone and rod system abnormality. mfERG findings were categorized based on the responses from central and paracentral hexagons into 2 subgroups: 1 - preserved central response surrounded by paracentral reduction; 2 - central and paracentral loss of responses.

Tartu, Estonia) in all probands.[43] The term "variants" used herein includes those sequence changes previously shown to be enriched in patients with Stargardt disease from prior studies. Null variants are those that would be expected to affect splicing, or to introduce a premature truncating codon in the protein if translated. Non-null variants (missense and in-frame deletions or insertions) were analyzed using 3 software prediction programs: SIFT (Sorting Intolerant from Tolerance; http://sift.jcvi.org/, accessed March 1, 2013),[44] PolyPhen2 (http://genetics.bwh.harvard.edu/pph/index.html, accessed March 1, 2013),[45] and the Human Splicing finder program version 2.4.1 (http://www.umd.be/HSF/, accessed March 1, 2013). Minor allele frequency for each allele was estimated with reference to the Exome Variant Server (NHLBI Exome Sequencing Project, Seattle, Washington, USA; http://snp.gs.washington.edu/EVS/, accessed March 1, 2013).

To investigate potential molecular genetic differences between patients with the foveal-sparing phenotype and those with typical disease (without foveal sparing/with foveal atrophy), the molecular data of patients with typical Stargardt disease ascertained at Moorfields Eye Hospital were reviewed. This comparison group consisted of all patients without evidence of foveal sparing on AF imaging and also harbored at least 1 *ABCA4* disease-causing variant following screening with the APEX microarray. One hundred and forty subjects from a total cohort of 438 individuals fulfilled these criteria, and the allele frequency of the most prevalent variants was compared between the group of patients with the foveal-sparing phenotype (n = 31) and the group of patients with typical Stargardt disease (n = 140).

RESULTS

THE CLINICAL FINDINGS IN THE 40 PATIENTS WITH FOVEAL-sparing Stargardt disease are summarized in Table 1. There were 22 female patients (55%) and 18 male patients (45%). The panel included 2 sibships; a sibling pair (Patients 16 and 32) and 1 set of 3 siblings (Patients 33, 34, and 35). Twenty-five patients (63%) complained of central visual loss and 2 subjects (5%) presented with diplopia, with 13 individuals (32%) having no visual symptoms. The median age of onset was 43.5 years (range, 25-75 years), and the median age at the examination was 46.5 years (range, 25-75 years). Nineteen patients (47.5%) had onset at ≥45 years of age. The mean duration of disease was 4.1 years (range, 0-25 years). The median logMAR visual acuity was 0.18 in the right eye and 0.18 in the left eye (range,

TABLE 1. Summary of Clinical Findings and Molecular Status of 40 Patients With a Foveal-Sparing Phenotype[a] of Stargardt Disease

						OCT			ERG[e]					
			LogMAR Visual Acuity			CFT[d] (μm)				PERG		mfERG		
Patient	Onset[b] (y)	Age (y)	OD	OS	Fundus Pattern[c]	OD	OS	ORT	Group	OD	OS	OD	OS	Mutation Status
1	45	45	0	0	3	219	223		NA	NA	NA	NA	NA	[c.1411 G>A, p.Glu471Lys/c.2588 G>C, p. Gly863Ala/c.4594 G>A, p.Asp1532Asn/c.5693 G>A, p.Arg1898His]
2	33	33	0.18	0.48	1	NA	NA		3	ND	ND	NA	NA	[c.1622 T>C, p.Leu541Pro/c.3113 C>T, p.Ala1038Val/c.6089 G>A, p.Arg2030Gln]
3	53	66	0.18	0.18	1	NA	NA		2	A	A	NA	NA	[c.768 G>T, Splice site/c. 6320 G>A, p. Arg2107His]
4	37	54	1.48	0.18	1	32	39	✓	3	ND	ND	2	2	[c.1760 +1 G>T, Splice site/c.4594 G>T, p.Asg1532Tyr]
5	57	57	0.3	0.18	1	NA	NA		1	ND	ND	NA	NA	[c. 1805G>A, p. Arg602Gln/c.3898 C>T, p.Arg1300*]
6	65*	65	0.18	0	1	211	187	✓	1	N	N	NA	NA	[c.5461-10 T>C, Splice site/c. 6089 G>A, p.Arg2030Gln]
7	54*	54	0	0	1	189	198		1	A	A	NA	NA	[c. 6089 G>A, p.Arg2030Gln/c.6118 C>T, p.Arg2040*]
8	39	44	−0.1	−0.1	4	297	230	✓	3	A	A	NA	NA	[c.71 G>A, p.Arg24His/c.4577 C>T, p. Thr1526Met]
9	35*	35	0.18	0.18	2	142	154		3	ND	ND	NA	NA	[c.658 C>T, p.p.Arg220Cys/c.2588 G>C, p. Gly863Ala]
10	45	54	0.48	0.18	1	102	116		3	ND	A	NA	NA	[c.1957 C>T, p.Arg653Cys/c.5693 G>A, p.Arg1898His]
11	43	43	−0.1	0	2	170	185		1	A	A	2	2	[c.2588 G>C, p. Gly863Ala/c.4139 C>T, p.Ala1038Val]
12	36**	38	0.3	0	1	220	212	✓	1	A	A	1	1	[c.4139 C>T, p.Ala1038Val/c.4594 G>T, p.Asp1532Asn]
13	62	68	−0.1	0.48	1	196	189	✓	1	N	N	2	2	[c.4222 T>C, p.Trp1408Arg/c.4918 C>T, p.Arg1640Trp]
14	36	44	0.48	0.48	3	79	89		1	A	A	NA	NA	[c.4222 T>C, p.Trp1408Arg/c.4918 C>T, p.Arg1640Trp]
15	46*	46	−0.1	−0.1	3	NA	NA		1	A	A	NA	NA	[c.4469 G>A, p.Cys1490Tyr/c. 6089 G>A, p.Arg2030Gln]
16	44*	44	0.18	0	2	NA	NA		1	A	A	NA	NA	[c.6079 C>T, p.Leu2027Phe/c.6079 C>T, p.Leu2027Phe]
17	48	73	0.18	3	4	135	86	✓	2	A	ND	NA	NA	[c.4956 T>G, p.Tyr1652*]
18	56	57	0	0	2	254	273		1	ND	A	NA	NA	[c.5018+2 T>C, Splice site]
19	53*	53	0.48	0.18	1	137	133		1	A	A	NA	NA	[c.5461-10 T>C, Splice site]
20	49	58	0.18	0	1	256	222	✓	1	A	N	1	1	[c.5461-10 T>C, Splice site]
21	47**	47	0.3	0.3	1	239	202	✓	1	A	A	1	1	[c.1805 G>A, p.Arg602Gln]
22	50*	50	0.48	0.18	1	263	261	✓	1	N	N	NA	NA	[c.1957 C>T, p.Arg653Cys]
23	39*	39	0	−0.1	2	225	228		1	N	N	NA	NA	[c.2588 G>C, p. Gly863Ala]
24	55	57	0.48	0.48	1	117	74		1	ND	ND	NA	NA	[c.3602 T>G, p.Leu1201Arg]
25	50	54	0.48	0.18	1	147	144	✓	3	ND	ND	NA	NA	[c.3602 T>G, p.Leu1201Arg]
26	43	47	2	0.18	1	70	52		1	ND	ND	NA	NA	[c.4319 T>C, p.Phe1440Ser]
27	30	51	0.3	0.3	1	75	79	✓	3	A	A	NA	NA	[c.4685 T>C, p.Ile1562Thr]
28	29	34	0.18	0.18	3	132	107		1	A	A	NA	NA	[c.4926 C>G, p.Ser1642Arg]
29	52*	52	0.18	0.18	3	180	200		1	ND	ND	2	2	[c.5882 G>A, p.Gly1961Glu]
30	28	28	−0.1	−0.1	2	NA	NA		1	N	ND	NA	NA	[c.6079 C>T, p.Leu2027Phe]
31	40*	40	−0.1	−0.1	2	222	223	✓	NA	NA	NA	NA	NA	[c.6079 C>T, p.Leu2027Phe]
32	45	48	0.18	3	1	237	252	✓	NA	NA	NA	NA	NA	NA

Continued on next page

central retinal atrophy.[13,15] Foveal-sparing forms of Stargardt disease may thus reflect a distinct pathogenesis.

The present study describes the clinical findings and molecular genetic characteristics of "foveal-sparing" Stargardt disease in a large cohort from a single center. The molecular data of the cohort with the foveal-sparing phenotype are compared with *ABCA4* variants observed in patients with Stargardt disease but without foveal sparing.

METHODS

• PATIENTS: AF images of the right eyes of 438 individuals with a clinical diagnosis of retinopathy compatible with Stargardt disease were surveyed and 40 patients were identified with an apparently normal AF signal at the fovea (foveal sparing). After informed consent, blood samples were collected and genomic DNA was extracted from the peripheral blood leukocytes. The protocol of the study adhered to the provisions of the Declaration of Helsinki and was approved by the local Ethics Committee of Moorfields Eye Hospital.

For the purposes of this report, patients presenting to the hospital with signs of atrophy within the macula, bilaterally, with or without surrounding flecks were potentially included as having Stargardt disease. Patients with a stationary visual dysfunction were excluded. A careful drug history was taken to allow exclusion of those with retinotoxic maculopathy. Patients with a dominant family history were excluded. Where a family history was not extensive, or whenever 2 generations were affected, the *RDS/PRPH2* gene, with its coding region and intron-exon boundaries, was sequenced. In those patients over 50 years of age, care was taken not to include cases of atrophic age-related macular degeneration in which there were soft drusen, or patients with maternally inherited diabetes and deafness in whom the distribution of atrophy and autofluorescence appearance had a distinctive appearance. The m.3243A>G variant was assayed if this phenotype was in any way suggested.

• CLINICAL ASSESSMENT: A detailed medical history was obtained and a comprehensive ophthalmologic examination was performed for all 40 patients. The age of onset was defined as the age at which visual loss was first noted by the patient or as the age at the latest examination for asymptomatic patients. The duration of the disease was calculated as the difference between age at onset and age at the latest examination. Assessment included best-corrected visual acuity, dilated ophthalmoscopy, color fundus photography, AF imaging, SDOCT imaging, and electrophysiological assessment. Best-corrected Snellen visual acuity was converted to equivalent logMAR visual acuity.

Color fundus photography was performed with a TRC-50IA retinal fundus camera (Topcon, Tokyo, Japan). AF images before 2009 were obtained with an HRA 2 (Heidelberg Engineering, Heidelberg, Germany; excitation light 488 nm; barrier filter 500 nm; field of view 30 × 30 degres),[34] and images after 2009 were undertaken using the Spectralis with viewing module version 5.1.2.0 (Heidelberg Engineering; excitation light 488 nm; barrier filter 500 nm; fields of view 30 × 30 degrees and 55 × 55 degrees).[35]

SDOCT was undertaken with the Spectralis with viewing module version 5.1.2.0. The SDOCT protocol included a horizontal linear scan (100 B-scans averaged to improve the signal-to-noise ratio) centered on the fovea, where possible, and a volume scan (minimum of 19 B-scan slices, 20 × 20 degrees). The HEYEX software interface (version 1.6.2.0; Heidelberg Engineering) was used for retinal thickness measurement.[36] Central foveal thickness was defined as the distance between the inner retinal surface and the inner border of the RPE.[36,37] Evidence of outer retinal tubulation was assessed from all the B-scan slices of each eye by 2 authors (K.F. and A.R.W.).[35,38]

• ELECTROPHYSIOLOGY: Electrophysiological assessment included full-field electroretinogram (ERG) and pattern electroretinogram (PERG) recorded with gold foil electrodes that incorporated the standards of the International Society for Clinical Electrophysiology of Vision.[39–41] The full-field ERGs were used to assess generalized rod and cone system function and included: (1) dark-adapted dim flash 0.01 candela-seconds per square meter ($cd \cdot s \cdot m^{-2}$); (2) dark-adapted bright flash 11.0 $cd \cdot s \cdot m^{-2}$; (3) light-adapted 3.0 $cd \cdot s \cdot m^{-2}$ 30 Hz flicker; and (4) light-adapted 3.0 $cd \cdot s \cdot m^{-2}$ at 2 Hz. The PERG P50 component and multifocal electroretinogram (mfERG) were used to assess macular function. Some patients had mfERG recording (RETIscan System; Roland Consult, Wiesbaden, Germany) with a stimulus consisting of 61 scaled hexagons covering in total a visual field of 55 degrees, at a viewing distance of 33 cm.[42] All main components of the ERG and the PERG P50 component were used to classify patients into 3 groups; this is a partial modification of a previous report[9]: (1) patients with normal ERGs with or without a PERG P50 abnormality; (2) subjects with a PERG P50 abnormality and additional generalized cone-mediated ERG abnormality (assessed with photopic ERGs); and (3) individuals with a PERG P50 abnormality and generalized cone system electrophysiological abnormality and additional generalized rod-mediated ERG abnormality (assessed using scotopic ERGs).

• MUTATION SCREENING AND MOLECULAR GENETIC ANALYSIS: Blood samples were collected in EDTA tubes and DNA was extracted with a Nucleon Genomic DNA extraction kit (BACC2; Tepnel Life Sciences, Manchester, United Kingdom), or the Qiagen Gentra Puregene blood kit (Qiagen, Venlo, Netherlands). Mutation screening of *ABCA4* was performed with the arrayed primer extension (APEX) microarray (ABCR400 chip, Asper Ophthalmics,

Clinical and Molecular Analysis of Stargardt Disease With Preserved Foveal Structure and Function

KAORU FUJINAMI, PANAGIOTIS I. SERGOUNIOTIS, ALICE E. DAVIDSON, GENEVIEVE WRIGHT, RAVINDER K. CHANA, KAZUSHIGE TSUNODA, KAZUO TSUBOTA, CATHERINE A. EGAN, ANTHONY G. ROBSON, ANTHONY T. MOORE, GRAHAM E. HOLDER, MICHEL MICHAELIDES, AND ANDREW R. WEBSTER

• PURPOSE: To describe a cohort of patients with Stargardt disease who show a foveal-sparing phenotype.
• DESIGN: Retrospective case series.
• METHODS: The foveal-sparing phenotype was defined as foveal preservation on autofluorescence imaging, despite a retinopathy otherwise consistent with Stargardt disease. Forty such individuals were ascertained and a full ophthalmic examination was undertaken. Following mutation screening of *ABCA4*, the molecular findings were compared with those of patients with Stargardt disease but no foveal sparing.
• RESULTS: The median age of onset and age at examination of 40 patients with the foveal-sparing phenotype were 43.5 and 46.5 years. The median logMAR visual acuity was 0.18. Twenty-two patients (22/40, 55%) had patchy parafoveal atrophy and flecks; 8 (20%) had numerous flecks at the posterior pole without atrophy; 7 (17.5%) had mottled retinal pigment epithelial changes; 2 (5%) had multiple atrophic lesions, extending beyond the arcades; and 1 (2.5%) had a bull's-eye appearance. The median central foveal thickness assessed with spectral-domain optical coherence tomographic images was 183.0 μm (n = 33), with outer retinal tubulation observed in 15 (45%). Twenty-two of 33 subjects (67%) had electrophysiological evidence of macular dysfunction without generalized retinal dysfunction. Disease-causing variants were found in 31 patients (31/40, 78%). There was a higher prevalence of the variant p.Arg2030Gln in the cohort with foveal sparing compared to the group with foveal atrophy (6.45% vs 1.07%).
• CONCLUSIONS: The distinct clinical and molecular characteristics of patients with the foveal-sparing phenotype are described. The presence of 2 distinct phenotypes of Stargardt disease (foveal sparing and foveal atrophy) suggests that there may be more than 1 disease mechanism in *ABCA4* retinopathy. (Am J Ophthalmol 2013;156: 487–501. © 2013 by Elsevier Inc. All rights reserved.)

Accepted for publication May 6, 2013.

From University College London, Institute of Ophthalmology, London, United Kingdom (K.F., P.I.S., A.E.D., G.W., R.K.C., C.A.E., A.G.R., A.T.M., G.E.H., M.M., A.R.W.); Moorfields Eye Hospital, London, United Kingdom (K.F., P.I.S., A.E.D., G.W., R.K.C., C.A.E., A.G.R., A.T.M., G.E.H., M.M., A.R.W.); Laboratory of Visual Physiology, National Institute of Sensory Organs, National Tokyo Medical Center, Tokyo, Japan (K.F., K.Tsunoda); and Department of Ophthalmology, Keio University, School of Medicine, Tokyo, Japan (K.F., K.Tsubota).

Inquiries to Professor Andrew R. Webster, University College London, Institute of Ophthalmology, 11-43 Bath Street, London EC1V 9EL, United Kingdom; e-mail: andrew.webster@ucl.ac.uk

STARGARDT DISEASE IS AN AUTOSOMAL RECESSIVE disorder caused by mutations in the *ABCA4* gene.[1,2] It is the most common single-gene retinal degeneration, with a reported prevalence of 1:10 000.[3,4] Most cases typically present with central visual loss within the first 2 decades of life, and during the course of the disorder there is macular atrophy with yellow-white flecks in the posterior pole, at the level of the retinal pigment epithelium (RPE).[4,5] However, Stargardt disease is associated with a variable phenotype and severity.[4–13] Autofluorescence (AF) imaging and electroretinography may assist the diagnosis, and parameters such as age of onset, visual acuity, AF pattern, and the nature of the electrophysiological findings assist both in the determination of disease severity and in the provision of prognostic information.[5,8,9,11,14] Increasingly, high-resolution imaging using spectral-domain optical coherence tomography (SDOCT) is providing insights into the retinal architectural changes that occur in Stargardt disease.[12,14–19]

There is wide phenotypic variability in *ABCA4* retinopathy[3,4,6,8,10,12,20–24] and sequence variants in *ABCA4* have also been implicated in cone dystrophy, cone-rod dystrophy, and "retinitis pigmentosa" in addition to Stargardt disease.[2,21,25–28] There is also extensive allelic heterogeneity, with more than 700 sequences in the *ABCA4* gene having been reported to date.[2,3,6,8,10,12,20–22,25–27,29,30-33] The phenotypic variability and the high genetic heterogeneity have confounded attempts to examine genotype-phenotype correlations comprehensively.[4,31,32]

A cohort of Stargardt disease patients who had better visual acuity than "typical" Stargardt disease patients, and who showed sparing of the fovea on funduscopy, has been described.[5] There are also reports of patients with "late-onset" Stargardt disease, including individuals with a foveal-sparing phenotype, who harbor *ABCA4* variants.[6,12,22] In those reports, SDOCT images demonstrated a well-preserved foveal structure including the neurosensory retina,[6,12,22] which differed from previous observations of early foveal photoreceptor damage in "typical" Stargardt disease with

0002-9394/$36.00
http://dx.doi.org/10.1016/j.ajo.2013.05.003

macular degeneration or cone-rod degeneration. *Invest Ophthalmol Vis Sci.* 2001;42:2229-2236.

20. Fumagalli A, Ferrari M, Soriani N, et al. Mutational scanning of the ABCR gene with double-gradient denaturing-gradient gel electrophoresis (DG-DGGE) in Italian Stargardt disease patients. *Hum Genet.* 2001;109:326-338.
21. Shroyer NF, Lewis RA, Yatsenko AN, Wensel TG, Lupski JR. Cosegregation and functional analysis of mutant ABCR (ABCA4) alleles in families that manifest both Stargardt disease and age-related macular degeneration. *Hum Mol Genet.* 2001; 10:2671-2678.
22. Klevering BJ, Blankenagel A, Maugeri A, Cremers FP, Hoyng CB, Rohrschneider K. Phenotypic spectrum of autosomal recessive cone-rod dystrophies caused by mutations in the ABCA4 (ABCR) gene. *Invest Ophthalmol Vis Sci.* 2002;43: 1980-1985.
23. Pang CP, Lam DS. Differential occurrence of mutations causative of eye diseases in the Chinese population. *Hum Mutat.* 2002;19:189-208.
24. Stenirri S, Fermo I, Battistella S, et al. Denaturing HPLC profiling of the ABCA4 gene for reliable detection of allelic variations. *Clin Chem.* 2004;50:1336-1343.
25. Downs K, Zacks DN, Caruso R, et al. Molecular testing for hereditary retinal disease as part of clinical care. *Arch Ophthalmol.* 2007;125:252-258.
26. Ernest PJ, Boon CJ, Klevering BJ, Hoefsloot LH, Hoyng CB. Outcome of ABCA4 microarray screening in routine clinical practice. *Mol Vis.* 2009;15:2841-2847.
27. Xi Q, Li L, Traboulsi EI, Wang QK. Novel ABCA4 compound heterozygous mutations cause severe progressive autosomal recessive cone-rod dystrophy presenting as Stargardt disease. *Mol Vis.* 2009;15:638-645.
28. Littink KW, Koenekoop RK, van den Born LI, et al. Homozygosity mapping in patients with cone-rod dystrophy: novel mutations and clinical characterizations. *Invest Ophthalmol Vis Sci.* 2010;51:5943-5951.
29. Maugeri A, van Driel MA, van de Pol DJ, et al. The 2588G->C mutation in the ABCR gene is a mild frequent founder mutation in the Western European population and allows the classification of ABCR mutations in patients with Stargardt disease. *Am J Hum Genet.* 1999;64:1024-1035.
30. Klevering BJ, Yzer S, Rohrschneider K, et al. Microarray-based mutation analysis of the ABCA4 (ABCR) gene in autosomal recessive cone-rod dystrophy and retinitis pigmentosa. *Eur J Hum Genet.* 2004;12:1024-1032.
31. Fujinami K, Sergouniotis PI, Davidson AE, et al. The clinical effect of homozygous ABCA4 alleles in 18 patients [published online ahead of print June 11, 2013]. *Ophthalmology.* doi:10.1016/j.ophtha.2013.04.016.
32. Sergouniotis PI, Davidson AE, Lenassi E, Devery SR, Moore AT, Webster AR. Retinal structure, function, and molecular pathologic features in gyrate atrophy. *Ophthalmology.* 2012; 119:596-605.
33. Bach M, Brigell MG, Hawlina M, et al. ISCEV standard for clinical pattern electroretinography (PERG): 2012 update. *Doc Ophthalmol.* 2013;126:1-7.
34. Marmor MF, Fulton AB, Holder GE, Miyake Y, Brigell M, Bach M. ISCEV standard for full-field clinical electroretinography (2008 update). *Doc Ophthalmol.* 2009;118:69-77.
35. Lois N, Holder GE, Bunce C, Fitzke FW, Bird AC. Phenotypic subtypes of Stargardt macular dystrophy-fundus flavimaculatus. *Arch Ophthalmol.* 2001;119:359-369.
36. Ng PC, Henikoff S. SIFT: predicting amino acid changes that affect protein function. *Nucleic Acids Res.* 2003;31:3812-3814.
37. Adzhubei IA, Schmidt S, Peshkin L, et al. A method and server for predicting damaging missense mutations. *Nat Methods.* 2010;7:248-249.
38. den Dunnen JT, Antonarakis SE. Mutation nomenclature extensions and suggestions to describe complex mutations: a discussion. *Hum Mut.* 2000;15:7-12.
39. Braun TA, Mullins RF, Wagner AH, et al. Non-exomic and synonymous variants in ABCA4 are an important cause of Stargardt disease. *Hum Mol Genet.* In press.
40. Burke TR, Allikmets R, Smith RT, Gouras P, Tsang SH. Loss of peripapillary sparing in non-group I Stargardt disease. *Exp Eye Res.* 2010;91:592-600.
41. Fritsche LG, Fleckenstein M, Fiebig BS, et al. A subgroup of age-related macular degeneration is associated with monoallelic sequence variants in the ABCA4 gene. *Invest Ophthalmol Vis Sci.* 2012;53:2112-2118.

the fovea in one patient, and a lack of peripapillary sparing on AF imaging in three subjects. In this study, patients with bilateral macular atrophy, with or without surrounding flecks, potentially were included as having Stargardt disease, with other less typical ("atypical") findings also having been reported in *ABCA4*-associated retinal disease.[18,40,41] However, other genes associated with autosomal recessive macular dystrophy, autosomal recessive cone-rod dystrophy, and autosomal recessive retinitis pigmentosa also should be considered for these patients with no identified likely disease-causing *ABCA4* alleles, in addition to the possibility of missed *ABCA4* alleles due to the inherent limitations of the molecular testing approach.

In our cohort, in keeping with previous reports, there was one well-known intronic variant (c.5461-10T>C) of equivocal pathogenicity following detailed in silico analysis,[4,5,16]; highlighting the need for an effective assay to determine functionally the effects of *ABCA4* variants, or alternatively to consider investigating mRNA expression. The allele, c.5461-10T>C, was the most common in our cohort, with 8/79 patients (10%) harboring this variant. Interestingly, the second allele was not identified in six of these patients. However, co-segregation of c.5461-10T>C with the disease has been documented in several studies, thereby strongly suggesting its disease-causation.[4]

In summary, we have demonstrated the validity and utility of *ABCA4* mutation screening with an NGS-based protocol in a large British cohort, with successful identification of the new disease-causing alleles in approximately half of the cases harboring one allele detected by prescreening with APEX technology. The identification of both disease-causing alleles will improve the accuracy of diagnosis and the counselling of patients, and also will assist in more effective patient selection of genetically confirmed participants for current and future clinical trials for *ABCA4*-associated retinal disease.

Acknowledgments

The authors thank the patients who kindly agreed to take part in this study and colleagues who referred individuals to us at Moorfields Eye Hospital, and those who contributed to the assembly of the *ABCA4* panel, particularly Naushin Waseem, Bev Scott, and Sophie Devery. The authors also thank Graham E. Holder, Anthony G. Robson, and Magella M. Neveu for interpretation of electrophysiologic data, and Yozo Miyake, Arundhati Dev Borman, Rajarshi Mukherjee, Eva Lenassi, Panagiotis I. Sergouniotis, and Aman Chandra for their insightful comments.

Supported by grants from the National Institute for Health Research Biomedical Research Centre at Moorfields Eye Hospital NHS Foundation Trust and UCL Institute of Ophthalmology; Foundation Fighting Blindness (USA); Fight For Sight; Moorfields Eye Hospital Special Trustees; Macular Disease Society; National Eye Institute/NIH Grants EY021163, EY019861, and EY019007 (Core Support for Vision Research); unrestricted funds from Research to Prevent Blindness (New York, NY) to the Department of Ophthalmology; Columbia University; Suzuken Memorial Foundation; Mitsukoshi Health and Welfare Foundation; Daiwa Anglo-Japanese Foundation; and Grant-in-Aid for Young Scientists (B) of the Ministry of Education, Culture, Sports, Science, and Technology (Japan); and by a Foundation Fighting Blindness Career Development Award (MM). The authors alone are responsible for the content and writing of the paper.

Disclosure: **K. Fujinami**, None; **J. Zernant**, None; **R.K. Chana**, None; **G.A. Wright**, None; **K. Tsunoda**, None; **Y. Ozawa**, None; **K. Tsubota**, None; **A.R. Webster**, None; **A.T. Moore**, None; **R. Allikmets**, None; **M. Michaelides**, None

References

1. Allikmets R, Singh N, Sun H, et al. A photoreceptor cell-specific ATP-binding transporter gene (ABCR) is mutated in recessive Stargardt macular dystrophy. *Nat Genet.* 1997;15:236-246.
2. Michaelides M, Chen LL, Brantley MA Jr, et al. ABCA4 mutations and discordant ABCA4 alleles in patients and siblings with bull's-eye maculopathy. *Br J Ophthalmol.* 2007;91:1650-1655.
3. Burke TR, Tsang SH. Allelic and phenotypic heterogeneity in ABCA4 mutations. *Ophthalmic Genet.* 2011;32:165-174.
4. Fujinami K, Lois N, Davidson AE, et al. A longitudinal study of Stargardt disease: clinical and electrophysiological assessment, progression and genotype correlations. *Am J Ophthalmol.* 2013;155:1075-1088.
5. Zernant J, Schubert C, Im KM, et al. Analysis of the ABCA4 gene by next-generation sequencing. *Invest Ophthalmol Vis Sci.* 2011;52:8479-8487.
6. Fujinami K, Akahori M, Fukui M, Tsunoda K, Iwata T, Miyake Y. Stargardt disease with preserved central vision: identification of a putative novel mutation in ATP-binding cassette transporter gene. *Acta Ophthalmol.* 2011;89:297-298.
7. Webster AR, Heon E, Lotery AJ, et al. An analysis of allelic variation in the ABCA4 gene. *Invest Ophthalmol Vis Sci.* 2001;42:1179-1189.
8. Cremers FP, van de Pol DJ, van Driel M, et al. Autosomal recessive retinitis pigmentosa and cone-rod dystrophy caused by splice site mutations in the Stargardt's disease gene ABCR. *Hum Mol Genet.* 1998;7:355-362.
9. Martinez-Mir A, Paloma E, Allikmets R, et al. Retinitis pigmentosa caused by a homozygous mutation in the Stargardt disease gene ABCR. *Nat Genet.* 1998;18:11-12.
10. Rozet JM, Gerber S, Souied E, et al. Spectrum of ABCR gene mutations in autosomal recessive macular dystrophies. *Eur J Hum Genet.* 1998;6:291-295.
11. Lewis RA, Shroyer NF, Singh N, et al. Genotype/phenotype analysis of a photoreceptor-specific ATP-binding cassette transporter gene, ABCR, in Stargardt disease. *Am J Hum Genet.* 1999;64:422-434.
12. Rozet JM, Gerber S, Ghazi I, et al. Mutations of the retinal specific ATP binding transporter gene (ABCR) in a single family segregating both autosomal recessive retinitis pigmentosa RP19 and Stargardt disease: evidence of clinical heterogeneity at this locus. *J Med Genet.* 1999;36:447-451.
13. Yatsenko AN, Shroyer NF, Lewis RA, Lupski JR. Late-onset Stargardt disease is associated with missense mutations that map outside known functional regions of ABCR (ABCA4). *Hum Genet.* 2001;108:346-355.
14. Jaakson K, Zernant J, Kulm M, et al. Genotyping microarray (gene chip) for the ABCR (ABCA4) gene. *Hum Mutat.* 2003;22:395-403.
15. Fishman GA, Stone EM, Grover S, Derlacki DJ, Haines HL, Hockey RR. Variation of clinical expression in patients with Stargardt dystrophy and sequence variations in the ABCR gene. *Arch Ophthalmol.* 1999;117:504-510.
16. Papaioannou M, Ocaka L, Bessant D, et al. An analysis of ABCR mutations in British patients with recessive retinal dystrophies. *Invest Ophthalmol Vis Sci.* 2000;41:16-19.
17. Rivera A, White K, Stohr H, et al. A comprehensive survey of sequence variation in the ABCA4 (ABCR) gene in Stargardt disease and age-related macular degeneration. *Am J Hum Genet.* 2000;67:800-813.
18. Birch DG, Peters AY, Locke KL, Spencer R, Megarity CF, Travis GH. Visual function in patients with cone-rod dystrophy (CRD) associated with mutations in the ABCA4(ABCR) gene. *Exp Eye Res.* 2001;73:877-886.
19. Briggs CE, Rucinski D, Rosenfeld PJ, Hirose T, Berson EL, Dryja TP. Mutations in ABCR (ABCA4) in patients with Stargardt

TABLE 6. Distribution of 79 Patients With *ABCA4*-Related Retinal Disease Based on Number of Identified Disease-Causing Variants

		Comprehensive Screening With APEX and NGS			
		No Disease-Causing Variant	1 Disease-Causing Variant	2 Disease-Causing Variants	3 Disease-Causing Variants
Prescreening with APEX	1 disease causing-variant, $n = 66$		29	36	1
	No disease-causing variants, $n = 13$	6	7		
	Total, $n = 79$	6	36	36	1

A total of 42 additional variants, which were not detected by APEX, were identified in 45 (57%) patients screened by NGS (Tables 2, 4). Three variants (p.R219*, p.R1108C, and p.S1071fs) found by NGS, were not identified by APEX at the prescreening stage despite being represented on the array ("APEX false-negative"; Table 2, patients 11, 16, 25, and 61). Three (3/45) subjects had two new variants and 42 (42/45) individuals had one new variant (Table 2). Of the 42 new variants detected by NGS, there were 23 missense, 9 splice-site alterations, 6 nonsense, 3 frameshifts, and 1 in-frame deletion (Table 4).

Of the 42 new variants identified by NGS, 33 (79%) were novel, including 18 missense, 7 splice-site alterations, 4 nonsense, 3 frameshifts, and 1 in-frame deletion (Tables 2, 4, 5). Seven variants identified only by NGS already were known, but not yet added to the *ABCA4* array by the time of the prescreening of those samples.

In Silico Molecular Genetic Analysis for New Variants Identified by NGS

In silico analysis of the 42 variants identified by NGS, including the 9 previously reported variants and the 33 novel variants, are shown in Tables 3 and 5, respectively.

Of the 9 previously reported variants that were detected by NGS, there were 4 null variants (2 nonsense and 2 splice-site alterations); 4 disease-causing missense variants, with deleterious or damaged protein function predicted by SIFT and Polyphen2; and one benign missense variant (p.D2177N, Table 3).

Deleterious or damaged protein function was predicted by SIFT and Polyphen2 in 16 of 18 novel missense variants (Table 5). Two variants (p.I478T and p.K896E) were predicted to be tolerated and benign. The predicted effects on splicing of these 16 missense variants, one variant resulting in a nucleotide substitution at the end of exon 33 (c.4773G>C), and five intronic variants, were assessed using the HSF program. Altered splicing was suggested for 7 of the missense variants, the (c.4773G>C) variant, and all 5 intronic variants (Table 5). The allele frequencies for the 33 novel variants were, at most, 1 in 13006, suggesting that these are all very rare. Overall, 31 of the 33 novel variants were considered disease-causing, except for only the two missense variants, p.I478T and p.K896E (Table 5).

Disease-Causing Variants

A total of 73 (31 novel and 42 previously identified) disease-causing variants was identified in this cohort of 79 patients (Table 4). The distribution of the number of alleles in the cohort is summarized in Table 6. One patient (1%) harbored three disease-causing variants, 36 (46%) had two disease-causing variants, 36 (46%) had one disease-causing variant, and six patients (7%) remained with no disease-causing variant identified (Table 6).

DISCUSSION

Our study reports the molecular genetic findings using a PCR-enrichment-based NGS strategy in a large well-characterized British cohort with a clinical diagnosis of *ABCA4*-associated retinal disease. The NGS revealed two or more disease-causing variants in 37 (47%) of 79 patients, in whom only one variant was detected in prescreening with APEX array technology.

Of the 66 subjects with one disease-causing allele identified previously by APEX, the second disease-causing allele was identified in 37 individuals (56%). In keeping with our findings, Zernant et al. reported that the same NGS strategy identified the second disease-causing allele in 48% of their cohort who also only had one allele found previously with APEX.[5] These findings suggest that many disease-associated mutations in the *ABCA4* gene are very rare and yet unknown, supporting the validity of the PCR-enrichment-based NGS method either as the screening method of choice, or as an additional screening method for patients in whom APEX does not reveal two variants. Of note, the NGS method is cost- and time-efficient at this time only for large (at least 96 samples) cohorts.

Of the 13 patients with initially no disease-causing variant found by APEX, one disease-causing *ABCA4* allele was identified in seven subjects (54%) by NGS, with six remaining with no likely disease-causing allele (46%). Further screening with NGS, including screening all intronic regions, and upstream and downstream control regions of the *ABCA4* gene, as well as other candidate genes, in larger well-characterized cohorts will be needed to identify fully all pathogenic alleles in these patients. It recently has been proposed that intronic and synonymous variants may account for a significant proportion of the remaining disease-causing variants not identified with exomic NGS.[5,39]

There were two "NGS false negative" variants (p.R1129H and p.Q1513fs) and three "APEX false negative" variants (p.R219*, p.R1108C, and p.S1071fs) in our cohort. The missense variant p.R1129H was not detected by NGS, most likely due to allele-specific amplification. The frameshift variant c.4537_4538insC, p.Q1513fs, is located in a homopolymer of seven C-nucleotides, where an insertion of another C nucleotide presents a challenge to identify by the Roche 454 sequencing platform. The "APEX false negative" variants were caused by technical issues with the specific array, ABCR400 (432 mutations on the chip) in 2005. Two of those variants, p.R1108C, and p.S1071fs, were detected by APEX in other patients (Table 2). Nevertheless, these findings suggest that combined APEX/NGS analysis may be worthy of consideration for comprehensive mutation detection.

In silico molecular genetic analysis was performed for all 84 variants identified in our cohort, with 73 of these determined to be likely disease-causing. Review of the clinical findings of the six patients harboring only one, likely benign, missense variant, revealed that they had a less typical ("atypical") phenotype for *ABCA4*-associated retinal disease, including an absence of flecks in all patients, significant peripheral retinal bone spicule pigmentation in three subjects, geographic-like atrophy in one individual, a subtle atrophic change confined to

TABLE 5. Continued

Exon/ IVS	DNA Change	Protein Change/ Effect	N of Alleles Identified	Pt	SIFT Pred.	SIFT Tol. Index (0–1)	Polyphen2 Pred.	Polyphen2 Hum Var Score (0–1)	HSF Matrix Site	HSF Matrix Wt CV	HSF Matrix Mt CV	HSF Matrix CV % Variation	Allele Freq. by EVS	Reference	Comments
33	c.4773G>C	Splice site	1	29					Don.	84.58	73.57	Site broken (−13.02)	ND		
35	c.4978delC	p.L1661*	1	24									ND		
36	c.5041_5055del GTGGTTGCCATCTGC	p.V1681_C1685del	1	40								NA	ND	db SNP (rs62646872)	
36	c.5088C>G	p.S1696R	1	10	Tol.	NA	PRD	0.780	Don.	59.34	86.17	New site (45.23)	ND		
39	c.5578C>T	p.R1860W	1	38	Del.	0.02	B	0.025				No change	ND	db SNP (rs200849015)	
IVS42	c.5899-3_ 5899-2delTA	Splice site	1	66								NA	ND		
IVS42	c.5899-2delA	Splice site	1	58					Acc.	82.1	28.26	WT site broken (−65.58)	ND		
45	c.6209C>G	p.T2070R	1	52	Tol.	NA	PRD	0.996	Acc.	57.41	86.36	New site (50.42)	ND		
46	c.6385A>G	p.S2129G	1	43	Del.	NA	B	0.001					ND		Possibly disease-causing

Splice-site alteration (described as splice site) includes the change expected to affect splicing, for example, when the splice donor or splice acceptor site is changed, and the change that might affect splicing, for example, changes close to the splice donor or splice acceptor site, or in the first or last nucleotide of an exon. SIFT (version 4.0.4) results are reported to be tolerant if tolerance index is ≥0.05 or deleterious if tolerance index is <0.05. Polyphen-2 (vision 2.1) appraises mutations qualitatively as benign, possibly damaging or probably damaging based on the model's false positive rate. The cDNA is numbered according to Ensemble transcript ID ENST00000370225, in which +1 is the A of the translation start codon. Human splicing finder version 2.4.1 was applied to predict the effect of each variant on splicing. The result from the HSF matrix indicates the values for the Wt and mutant sequences. The larger the difference in values between the Wt and the mutant sequences suggests a greater chance that the variant can affect splicing. EVS denotes variants in the Exome Variant Server, NHLBI Exome Sequencing Project, Seattle, WA (accessed 01/04/2013; available in the public domain at http://snp.gs.washington.edu/EVS).

Table 5. In Silico Molecular Genetic Analysis for Novel ABCA4 Variants Identified by NGS

					SIFT		Polyphen2		HSF Matrix						
Exon/ IVS	DNA Change	Protein Change/ Effect	*N* of Alleles Identified	Pt	Pred.	Tol. Index (0–1)	Pred.	Hum Var Score (0–1)	Site	Wt CV	Mt CV	CV % Variation	Allele Freq. by EVS	Reference	Comments
3	c.180delG	p.M61fs	1	35									ND		
IVS7	c.859-9T>C	Splice site	1	5					Acc.	78.18	76.99	Possibly site broken (−1.52)	ND		Possibly disease-causing
11	c.1433T>C	p.I478T	1	1	Tol.		B	0.007				No change	ND		Benign
11	c.1519G>T	p.D507Y	1	20	Del.	0.01	POD	0.641				No change	1/13006	dbSNP (rs148234178)	
12	c.1749G>C	p.K583N	1	68	Del.	0.04	POD	0.893	Acc.	66.17	37.22	Site broken (−43.75)	1/13006	dbSNP (rs145265791)	
14	c.1982_ 1983insG	p.A662fs	1	69									ND		
15	c.2297G>T	p.G766V	1	1	Tol.	NA	POD	0.557	Don.	69.18	42.34	Site broken (−38.79)	ND		
15	c.2345G>A	p.W782*	1	3									ND		
16	c.2510T>C	p.L837P	1	72	Tol.	NA	POD	0.905				No change	ND		
16	c.2568C>A	p.Y856*	1	5									ND		
18	c.2686A>G	p.K896E	1	53	Tol.	NA	B	0.002					ND		Benign
20	c.2942C>T	p.P981L	1	19	Del.	0.00	POD	0.813				No change	1/13006	dbSNP (rs147826775)	
20	c.2972G>T	p.G991V	1	70	Del.	NA	PRD	0.998	Donor	64.62	91.45	New site (41.53)	ND		
IVS20	c.3050+1G>C	Splice site	1	54					Acc.	86.43	57.49	Site broken (−33.49)	ND		
IVS21	c.3191-1G>T	Splice site	1	26					Acc.	94.38	65.44	WT site broken (−30.67)	ND		
22	c.3289A>T	p.R1097*	1	71									ND		
22	c.3299T>A	p.I1100N	1	23	Del.	NA	PRD	0.986				No change	ND		
23	c.3370G>T	p.D1124Y	1	62	Del.	NA	PRD	0.998				No change	ND		
23	c.3392delC/ 3393C>G	p.A1131Gfs	1	55									ND		
23	c.3398T>C	p.I1133T	1	27	Del.	NA	B	0.100				No change	ND		Possibly disease-causing
27	c.4070C>A	p.A1357E	1	28	Del.	NA	PRD	0.94	Acc.	40.92	69.86	New site (+70.74)	ND		
IVS30	c.4539+2T>G	Splice site	1	56					Don.	79.18	52.35	WT site broken (−33.89)	ND		
31	c.4552A>C	p.S1518R	1	57	Del.	NA	POD	0.871	Acc.	76.3	47.36	Site broken (−37.94)	ND		
31	c.4634G>A	p.S1545N	2	21, 25	Tol.	NA	B	0.253	Acc.	80.04	51.1	Site broken (−36.16)	ND		

TABLE 4. Numbers and Types of Variants Detected by APEX Technology and NGS

		Null				Non-Null		
	Total	Splice-Site Altering	Nonsense	Frameshift	Unknown	In-Frame Deletion	Disease-Causing Missense	Benign Missense
Variants detected by prescreening with APEX	42	4	4	2	1	0	23	8
New variants detected by NGS alone	42 (33)	9 (7)	6 (4)	3 (3)	0 (0)	1 (1)	20 (16)	3 (2)
Gross total	84 (33)	13 (7)	10 (4)	5 (3)	1 (0)	1 (1)	43 (16)	11 (2)

Numbers in parentheses indicate the numbers of novel variants that have never been reported. Two variants were detected only on APEX array, but not identified by NGS; one frameshift variant (p.Q1513fs) and one disease-causing missense variant (p.R1129H).

tional generalized cone and rod ERG abnormality (assessed using dark adapted 0.01 dim flash ERG and dark adapted 11.0 bright flash ERG).

Genetic Screening

Blood samples were collected in EDTA tubes and DNA was extracted with a Nucleon Genomic DNA extraction kit (BACC2; Tepnel Life Sciences, Manchester, UK). Mutation prescreening of *ABCA4* was performed with the APEX microarray (ABCR400 chip or ABCR600 chip; Asper Ophthalmics, Tartu, Estonia; available in the public domain at http://www.asperbio.com/genetic-tests/panel-of-genetic-tests/stargardt-disease-cone-rod-dystrophy-abca4) in all probands.[14] We screened 17 patients with ABCR400 (432 mutations on the chip) in 2005, 32 with updated ABCR400 (456 mutations) in 2006, 3 with further updated ABCR400 (480 mutations) in 2007, and 27 with ABCR500 (552 mutations) in 2011.

All 50 *ABCA4* exons and exon-intron boundaries were amplified with tagged PCR primers using an amplicon tagging protocol (Access Array; Fluidigm, South San Francisco, CA; available in the public domain at http://www.fluidigm.com/products/access-array.html) and NGS on the Roche 454 platform (Roche Applied Science, Penzberg, Upper Bavaria, Germany) was performed as reported previously.[5] Sequences of the barcoded samples were analyzed with the NextGENE software for next generation sequence analysis (SoftGenetics, State College, PA), which mapped reads to the reference genome (HG19) and identified all the differences compared to the reference sequence. All the identified variants were confirmed by Sanger sequencing. Segregation analysis was not performed in this study.

In Silico Molecular Genetic Analysis

All the missense variants identified were analyzed using two software prediction programs: Sorting Intolerant From Tolerant (SIFT; available in the public domain at http://sift.jcvi.org),[36] and PolyPhen2 (available in the public domain at http://genetics.bwh.harvard.edu/pph/index.html).[37] Predicted effects on splicing of all the missense and intronic variants were assessed with the Human Splicing Finder (HSF) program version 2.4.1 (available in the public domain at http://www.umd.be/HSF). The allele frequency of all the variants was estimated by reference to the Exome Variant Server (EVS; NHLBI Exome Sequencing Project, Seattle, WA; available in the public domain at http://snp.gs.washington.edu/EVS).

All the variants identified were classified into one of three categories based on the bioinformatics prediction protocol described in a previous report,[5] namely disease-causing, possibly disease-causing, and benign. For the purpose of analysis in this study, variants predicted to be possibly disease-causing were included in the total number of variants described as disease-causing variants. The nomenclature of the variants was in the main in keeping with the internationally established guidelines (available in the public domain at http://www.hgvs.org/mutnomen).[38]

RESULTS

Clinical Findings

The clinical findings of the cohort are summarized in Table 1. The study included 40 male (51%) and 39 female (49%) unrelated probands. The median age at onset was 22.0 years, with a median duration of disease of 10.0 years. The median age at the latest examination was 40.0 years, with the median logMAR visual acuities being 1.00. Color fundus photographs were obtained in 75 patients and AF imaging was undertaken in 71 subjects. There were 21 patients (30%) with a type 1 AF pattern, 34 (48%) with type 2, and 16 (22%) with type 3. Of the 70 patients with available electrophysiologic data, 34 subjects (49%) were in ERG group 1 (isolated macular dysfunction), 7 (10%) in ERG group 2 (macular and generalized cone dysfunction), and 29 (41%) in ERG group 3 (macular and generalized cone and rod dysfunction).

Color fundus photographs, AF images, and SD-OCT of three representative cases of "typical" *ABCA4*-associated retinal disease are shown in Figure 1 (patients 19, 36, and 17), all harboring two disease-causing variants. Six cases with an "atypical" phenotype for *ABCA4*-associated retinal disease are shown in Figure 2 (patients 74–79), all of them carried only one, likely benign, *ABCA4* variant (Table 2).

Prescreening With APEX Technology

The results of prescreening of *ABCA4* in our cohort of 79 patients are summarized in Table 2. We detected 42 variants at the APEX prescreening stage. In silico analysis of these 42 variants suggested that 34 were disease-causing and 8 were considered benign. Therefore, these analyses confirmed at least one disease-causing variant in 66/79 patients, while 13/79 subjects had no disease-causing variants (Tables 2, 3).

Identification of New Variants by NGS

The results of NGS screening in our cohort of 79 patients are summarized in Table 2. We identified 82 variants by NGS in total; 53 missense, 13 splice-site alterations, 10 nonsense, four frameshifts, one in-frame deletion, and one intronic variant of unknown effect (Tables 2, 4). Of a total of 84 different variants identified in this study by APEX and NGS, there were two "NGS false-negative" variants (p.R1129H and p.Q1513fs), which were detected on APEX array, but were not detected by NGS (Table 2, patients 25 and 38).

TABLE 3. Continued

Exon/ IVS	Nucleotide Substitution	Protein Change/ Effect	*N* of Alleles Identified	Pt	Method: APEX	Method: NGS	Previous Report	SIFT: Pred.	SIFT: Tol. Index (0–1)	Polyphen 2: Pred.	Polyphen 2: Hum Var Score (0–1)	HSF Matrix: Site	HSF Matrix: Wt CV	HSF Matrix: Mt CV	CV % Variation	Allele Freq. by EVS	Reference	Comment
30	c.4537_4538insC	p.G1513fs	1	38	✓		Briggs CE, et al.[19]									ND		False-negative in NGS in patient 38
31	c.4577C>T	p.T1526M	1	39	✓	✓	Lewis RA, et al.[11]	Del.	0.00	PRD	0.910				No change	ND	db SNP (rs61750152)	
33	c.4685T>C	p.I1562T	1	71	✓	✓	Yatsenko, et al.[13]	Tol.	NA	PRD	0.783				No change	ND		Benign
33	c.4715C>T	p.T1572M	1	79	✓	✓	Pang CP and Lamm DS[23]	Del.	0.02	B	0.326				No change	ND	db SNP (rs185093512)	Benign
35	c.4926C>G	p.S1642R	1	40	✓	✓	Birch DG, et al.[22]	Tol.	0.68	B	0.116				No change	ND	db SNP (rs61753017)	
35	c.4956T>G	p.Y1652*	1	41	✓	✓	Fumagalli A, et al.[16]									ND	db SNP (rs61750561)	
IVS35	c.5018+2T>C	Splice site	1	42	✓	✓	APEX					Don.	81.2	54.3	WT site broken (−33.07)	ND		
36	c.5113C>T	p.R1705W	1	7		✓	Ernest PJ, et al.[20]	Del.	NA	PRD	0.996	Don.	46.5	73.3	No change	ND		
IVS38	c.5461-10T>C		8	43, 44, 45, 46, 47, 48, 49, 50	✓	✓	Briggs CE, et al.[19]								No change	3/13006	db SNP (rs1800728)	
IVS39	c.5585-1G>A	Splice site	1	51	✓	✓	Shroyer NF, et al.[21]					Acc.	86.3	57.4	WT site broken (−33.53)	ND		
IVS40	c.5714+5G>A	Splice site	1	52	✓	✓	Cremers FP, et al.[8]					Don.	85.5	73.3	Wild type site broken (−14.23)	ND		
42	c.5882G>A	p.G1961E	7	53, 54, 55, 56, 57, 58, 59	✓	✓	Lewis RA, et al.[11]	Del.	0.00	PRD	0.998				No change	41/13006	db SNP (rs1800553)	
44	c.6079C>T	p.L2027F	4	60, 61, 62, 63	✓	✓	Lewis RA, et al.[11]	Del.	0.00	PRD	1.000				No change	4/13006	db SNP (rs61751408)	
44	c.6089G>A	p.R2030Q	1	64	✓	✓	Lewis RA, et al.[11]	Del.	0.00	PRD	0.995				No change	8/13006	db SNP (rs61750641)	
46	c.6320G>A	p.R2107H	2	72, 73	✓	✓	Fishman GA, et al.[15]	Del.	0.01	PRD	0.999				No change	91/13006	db SNP (rs62642564)	Benign
47	c.6445C>T	p.R2149*	1	65	✓	✓	Lewis RA, et al.[14]									1/13006	db SNP (rs61750654)	
48	c.6529G>A	p.D2177N	1	19		✓	Rivera A, et al.[17]	Tol.	0.41	B	0.004				No change	116/13006	db SNP (rs1800555)	Benign
48	c.6709A>C	p.T2237P	1	66	✓	✓	APEX	Del.	NA	POD	0.719				No change	ND		
IVS48	c.6729+1_ +18del AGTTGGCCCTGGGGC	Splice site	1	17		✓	Littink KW, et al.[28]								NA	ND		

Splice-site alteration (described as splice site) includes the change expected to affect splicing, for example, when the splice donor or splice acceptor site is changed, and the change that might affect splicing, for example, changes close to the splice donor or splice acceptor site, or in the first or last nucleotide of an exon. SIFT (version 4.0.4) results are reported to be tolerant if tolerance index is $\geq$0.05 or deleterious if tolerance index is <0.05. Polyphen-2 (vision 2.1) appraises mutations qualitatively as benign, possibly damaging or probably damaging based on the model's false positive rate. The cDNA is numbered according to Ensemble transcript ID ENST00000370225, in which +1 is the A of the translation start codon. Human splicing finder version 2.4.1 was applied to predict the effect of each variant on splicing. The result from the HSF matrix indicates the values for the wild type (Wt) and mutant sequences. The larger the difference in values between the Wt and the mutant sequences suggests a greater chance that the variant can affect splicing. EVS denotes variants in the Exome Variant Server, NHLBI Exome Sequencing Project, Seattle, WA (accessed 01/04/2013; available in the public domain at http://snp.gs.washington.edu/EVS). Acc., Acceptor; Allele freq., allele frequency; CV, consensus values; Del., deleterious; Don., donor; EVS, exome variant server; HSF, human splicing finder; IVS, intervening sequence; Mt, mutant; NA, not available; ND, not detected; POD, possibly damaging; PRD, probably damaging; Pred., prediction; Tol., tolerant.

TABLE 3. In Silico Analysis for Previously Reported Variants Identified in 79 Patients With ABCA4-Related Retinal Disease

					Method			SIFT		Polyphen 2		HSF Matrix							
Exon/ IVS	Nucleotide Substitution	Protein Change/ Effect	*N* of Alleles Identified	Pt	APEX	NGS	Previous Report	Pred.	Tol. Index (0–1)	Pred.	Hum Var Score (0–1)	Site	Wt CV	Mt CV	CV % Variation	Allele Freq. by EVS	Reference	Comment
3	c.161G>A	p.C54Y	1	1	✓	✓	Lewis RA, et al.[11]	Tol.	0.11	PRD	0.994				No change	1/13006	db SNP (rs150774447)	
3	c.223T>G	p.C75G	1	2	✓	✓	Lewis RA, et al.[11]	Del.	NA	POD	0.603				No change	ND		
5	c.466A>G	p.I156V	2	77, 78	✓	✓	Papaioannou M, et al.[16]	Tol.	0.46	B	0.003				No change	16/13006	db SNP (rs112467008)	Benign
6	c.655A>T	p.R219*	1	11		✓	Xi Q, et al.[27]									ND		
6	c.740A>C	p.N247T	1	3	✓	✓	APEX	Del.	NA	B	0.135				No change	ND		
6	c.768G>T	Splice site	1	4	✓	✓	Klevering BJ, et al.[22]	Tol.	0.56	NA		Don.	70.4	58	Site broken (−17.51)	ND		
9	c.1222C>T	p.R408*	1	5	✓	✓	Webster AR, et al.[7]									ND		
12	c.1726G>C	p.D576H	1	36		✓	Downs K, et al.[25]			POD	0.688	Acc.	68.1	39.1	Site broken (−42.54)	1/13006		
13	c.1804C>T	p.R602W	1	6	✓	✓	Lewis RA, et al.[11]	Del.	0.00	B	0.129				No change	ND	db SNP (rs 6179409)	
13	c.1805G>A	p.R602Q	1	7	✓	✓	Webster AR, et al.[7]	Del.	0.04	PRD	0.513	Acc.	48.9	77.9	New site (+59.14)	2/13006	db SNP (rs61749410)	
13	c.1906C>T	p.Q636*	3	12, 13, 60		✓	Zernant J, et al.[5]								No change	1/13006	db SNP (rs145961131)	
13	c.1922G>C	p.C641S	1	8	✓	✓	Stenirri S, et al.[24]	Del.	0.00						No change	ND	db SNP (rs61749416)	
14	c.1957C>T	p.R653C	2	9, 10	✓	✓	Rivera A, et al.[17]	Del.	0.00	PRD	0.999				No change	ND	db SNP (rs61749420)	
17	c.2588G>C	p.G863A/ p.DelG863	5	11, 12, 13, 14, 15	✓	✓	Lewis RA, et al.[11]/ Maugeri A, et al.[20]	Del.	0.00	PRD	0.996				No change	68/13006	db SNP (rs76157638)	
18	c.2701A>G	p.T901A	1	74	✓	✓	APEX	Tol.	0.82	B	0.008					23/13006	db SNP (rs149655975)	Benign
19	c.2894A>G	p.N965S	1	16	✓	✓	Lewis RA, et al.[11]	Del.	0.03	PRD	0.981	Acc.	53.4	82.3	New site (+54.26)	ND	db SNP (rs201471607)	
20	c.2971G>C	p.G991R	1	67	✓	✓	Yatsenko AN, et al.[15]	Del.	0.02	PRD	0.999				No change	28/13006	db SNP (rs147484266)	Benign
22	c.3064G>A	p.E1022K	2	17, 18	✓	✓	Webster AR, et al.[7]	Del.	0.00	PRD	1.000				No change	ND	db SNP (rs61749459)	
22	c.3208_3209insGT	p.S1071fs	5	19, 20, 21, 22, 25	✓	✓	APEX									ND		False-negative in APEX in patient 25
22	c.3292C>T	p.R1098C	1	23	✓	✓	Rivera A, et al.[17]	Del.	NA	PRD	0.999				No change	ND		
22	c.3322C>T	p.R1108C	3	16, 24, 61	✓	✓	Rozet JM, et al.[19]	Del.	0.00	PRD	0.986				No change	1/13006	db SNP (rs61750120)	False-negative in APEX in patients 16 and 61
23	c.3386G>A	p.R1129H	1	25	✓		Zernant J, et al.[5]			PRD	0.989				No change	ND		False-negative in NGS in patient 25
24	c.3602T>G	p.L1201R	4	72, 73, 74, 79	✓	✓	Lewis RA, et al.[11]	Tol.	0.37	B	0.052	Don.	61.3	73.7	New site (20.08)	416/13006	db SNP (rs61750126)	Benign
28	c.4139C>T	p.P1380L	7	30, 31, 32, 33, 34, 35, 36	✓	✓	Lewis RA, et al.[11]	Del.	0.01	B	0.377				No change	2/13006	db SNP (rs61750130)	
28	c.4234C>T	p.Q1412*	1	33	✓	✓	Rivera A, et al.[17]									ND	db SNP (rs61750137)	
29	c.4283C>T	p.T1428M	1	76	✓	✓	APEX	Tol.	0.15	B	0.010				No change	2/13006	db SNP (rs1800549)	Benign
29	c.4319T>C	p.F1440S	1	34	✓	✓	Lewis RA, et al.[11]	Del.	0.00	POD	0.744				No change	ND	dbSNP (rs61750141)	
29	c.4326C>A	p.N1442K	1	64		✓	Zernant J, et al.[5]	Tol.	NA	POD	0.374				No change	ND		
29	c.4328G>A	p.R1443H	1	35	✓	✓	Rivera A, et al.[17]	Del.	0.02	PRD	0.999				No change	1/13006	dbSNP (rs61750142)	
IVS29	c.4352+1G>A	Splice site	1	73		✓	Zernant J, et al.[5]					Don.	82.3	55.4	WT site broken (−32.62)	ND		
30	c.4469G>A	p.C1490Y	2	36, 37	✓	✓	Lewis RA, et al.[11]	Del.	0.00	PRD	0.994				No change	ND	dbSNP (rs61751402)	
30	c.4538A>G	p.Q1513R	1	67		✓	Webster AR, et al.[7]	Tol.	NA	Benign	0.043	Acc.	91.7	62.8	Site broken (−31.55)	ND		

TABLE 2. Continued

	Allele 1 Detected by APEX			Allele 2 Detected by NGS			Allele 3 Detected by NGS				
Pt	DNA Change	Protein Change/ Effect	Pred. Patho.	DNA Change	Protein Change/ Effect	Pred. Patho.	DNA Change	Protein Change/ Effect	Pred. Patho.	Total *N* of DC Variants	Comments
40	c.4926C>G	p.S1642R	DC	*c.5041_5055del GTGGTTGCCATCTGC*	*p.V1681_C1685del*	DC				2	
41	c.4956T>G	p.Y1652*	DC							1	
42	c.5018+2T>C	Splice site	DC							1	
43	c.5461-10T>C		DC	*c.6385A>G*	*p.S2129G*	PDC				2	
44	c.5461-10T>C		DC							1	
45	c.5461-10T>C		DC							1	
46	c.5461-10T>C		DC							1	
47	c.5461-10T>C		DC							1	
48	c.5461-10T>C		DC							1	
49	c.5461-10T>C		DC							1	
50	c.5461-10T>C		DC							1	
51	c.5585-1G>A	Splice site	DC							1	
52	c.5714+5G>A	Splice site	DC	*c.6209C>G*	*p.T2070R*	DC				2	
53	c.5882G>A	p.G1961E	DC	*c.2686A>G*	*p.K896E*	B				1	
54	c.5882G>A	p.G1961E	DC	*c.3050+1G>C*	*Splice site*	DC				2	
55	c.5882G>A	p.G1961E	DC	*c.3392delC/3393C>G*	*p.A1131Gfs*	DC				2	
56	c.5882G>A	p.G1961E	DC	*c.4539+2T>G*	*Splice site*	DC				2	
57	c.5882G>A	p.G1961E	DC	*c.4552A>C*	*p.S1518R*	DC				2	
58	c.5882G>A	p.G1961E	DC	*c.5899-2delA*	*Splice site*	DC				2	
59	c.5882G>A	p.G1961E	DC							1	
60	c.6079C>T	p.L2027F	DC	c.1906C>T	p.Q636*	DC				2	
61	c.6079C>T	p.L2027F	DC	c.3322C>T	p.R1108C	DC				2	Allele 2 (p.R1108C) was APEX-false-negative
62	c.6079C>T	p.L2027F	DC	*c.3370G>T*	*p.D1124Y*	DC				2	
63	c.6079C>T	p.L2027F	DC							1	
64	c.6089G>A	p.R2030Q	DC	c.4326C>A	p.N1442K	DC				2	
65	c.6445C>T	p.R2149*	DC							1	
66	c.6709A>C	p.T2237P	DC	*c.5899-3_5899-2delTA*	*Splice site*	DC				2	
67	c.2971G>C	p.G991R	B	c.4538A>G	p.Q1513R	DC				1	
68	c.3602T>G	p.L1201R	B	*c.1749G>C*	*p.K583N*	DC				1	
69	c.3602T>G	p.L1201R	B	*c.1982_1983insG*	*p.A662fs*	DC				1	
70	c.3602T>G	p.L1201R	B	*c.2972G>T*	*p.G991V*	DC				1	
71	c.4685T>C	p.I1562T	B	*c.3289A>T*	*p.R1097**	DC				1	
72	c.6320G>A	p.R2107H	B	*c.2510T>C*	*p.L837P*	DC				1	
73	c.6320G>A	p.R2107H	B	c.4352+1G>A	Splice site	DC				1	
74	c.2701A>G	p.T901A	B							0	
75	c.3602T>G	p.L1201R	B							0	
76	c.4283C>T	p.T1428M	B							0	
77	c.466A>G	p.I156V	B							0	
78	c.466A>G	p.I156V	B							0	
79	c.4715C>T	p.T1572M	B							0	

Putative novel variants are shown in italics. Splice-site alteration (described as splice site) includes the change expected to affect splicing, for example, when the splice donor or splice acceptor site is changed, and the change that might affect splicing, for example, changes close to the splice donor or splice acceptor site, or in the first or last nucleotide of an exon. Two variants result in nucleotide substitution at the end of an exon and cause splice-site alteration (c.768G>T and c.4773G>C). B, benign; DC, disease-causing; PDC, possibly disease-causing; Pred. Patho, predicted pathogenicity; Pt, patient number.

TABLE 2. Molecular Genetic Status Identified by NGS in 79 Patients With *ABCA4*-Related Retinal Disease

	Allele 1 Detected by APEX			Allele 2 Detected by NGS			Allele 3 Detected by NGS				
Pt	DNA Change	Protein Change/ Effect	Pred. Patho.	DNA Change	Protein Change/ Effect	Pred. Patho.	DNA Change	Protein Change/ Effect	Pred. Patho.	Total *N* of DC Variants	Comments
1	c.161G>A	p.C54Y	DC	*c.2297G>T*	*p.G766V*	DC				2	
2	c.223T>G	p.C75G	DC	*c.5088C>G*	*p.S1696R*	DC				2	
3	c.740A>C	p.N247T	DC	*c.1433T>C*	*p.I478T*	B	*c.2345G>A*	*p.W782**	DC	2	
4	c.768G>T	Splice site	DC							1	
5	c.1222C>T	p.R408*	DC	*c.2568C>A*	*p.Y856**	DC				2	
6	c.1804C>T	p.R602W	DC	*c.859-9T>C*	*Splice site*	PDC				2	
7	c.1805G>A	p.R602Q	DC	c.5113C>T	p.R1705W	DC				2	
8	c.1922G>C	p.C641S	DC							1	
9	c.1957C>T	p.R653C	DC							1	
10	c.1957C>T	p.R653C	DC							1	
11	c.2588G>C	p.G863A	DC	c.655A>T	p.R219*	DC				2	Allele 2 (p.R219*) was APEX-false-negative
12	c.2588G>C	p.G863A	DC	c.1906C>T	p.Q636*	DC				2	
13	c.2588G>C	p.G863A	DC	c.1906C>T	p.Q636*	DC				2	
14	c.2588G>C	p.G863A	DC							1	
15	c.2588G>C	p.G863A	DC							1	
16	c.2894A>G	p.N965S	DC	c.3322C>T	p.R1108C	DC				2	Allele 2 (p.R1108C) was APEX-false-negative
17	c.3064G>A	p.E1022K	DC	c.6729+4_+18delAGTTGGCCCTGGGGC	Splice site	DC				2	
18	c.3064G>A	p.E1022K	DC							1	
19	c.3208_3209insGT	p.S1071fs	DC	*c.2942C>T*	*p.P981L*	DC	c.6529G>A	p.D2177N	B	2	
20	c.3208_3209insGT	p.S1071fs	DC	*c.1519G>T*	*p.D507Y*	DC				2	
21	c.3208_3209insGT	p.S1071fs	DC	*c.4634G>A*	*p.S1545N*	DC				2	
22	c.3208_3209insGT	p.S1071fs	DC							1	
23	c.3292C>T	p.R1098C	DC	*c.3299T>A*	*p.I1100N*	DC				2	
24	c.3322C>T	p.R1108C	DC	*c.4978delC*	*p.L1661**	DC				2	
25	c.3386G>A	p.R1129H	DC	c.3208_3209insGT	p.S1071fs	DC	*c.4634G>A*	*p.S1545N*	DC	3	Allele 2 (p.S1071fs) was APEX false-negative and allele 1 (p.R1129H) was NGS false-negative
26	c.4139C>T	p.P1380L	DC	*c.3191-1G>T*	*Splice site*	DC				2	
27	c.4139C>T	p.P1380L	DC	*c.3398T>C*	*p.I1133T*	PDC				2	
28	c.4139C>T	p.P1380L	DC	*c.4070C>A*	*p.A1357E*	DC				2	
29	c.4139C>T	p.P1380L	DC	*c.4773G>C*	*Splice site*	DC				2	
30	c.4139C>T	p.P1380L	DC							1	
31	c.4139C>T	p.P1380L	DC							1	
32	c.4139C>T	p.P1380L	DC							1	
33	c.4234C>T	p.Q1412*	DC							1	
34	c.4319T>C	p.F1440S	DC							1	
35	c.4328G>A	p.R1443H	DC	*c.180delG*	*p.M61fs*	DC				2	
36	c.4469G>A	p.C1490Y	DC	c.1726G>C	p.D576H	DC				2	
37	c.4469G>A	p.C1490Y	DC							1	
38	c.4537_4538insC	p.Q1513fs	DC	*c.5578C>T*	*p.R1860W*	DC				2	Allele 1 (p.Q1513fs) was NGS-false-negative
39	c.4577C>T	p.T1526M	DC							1	

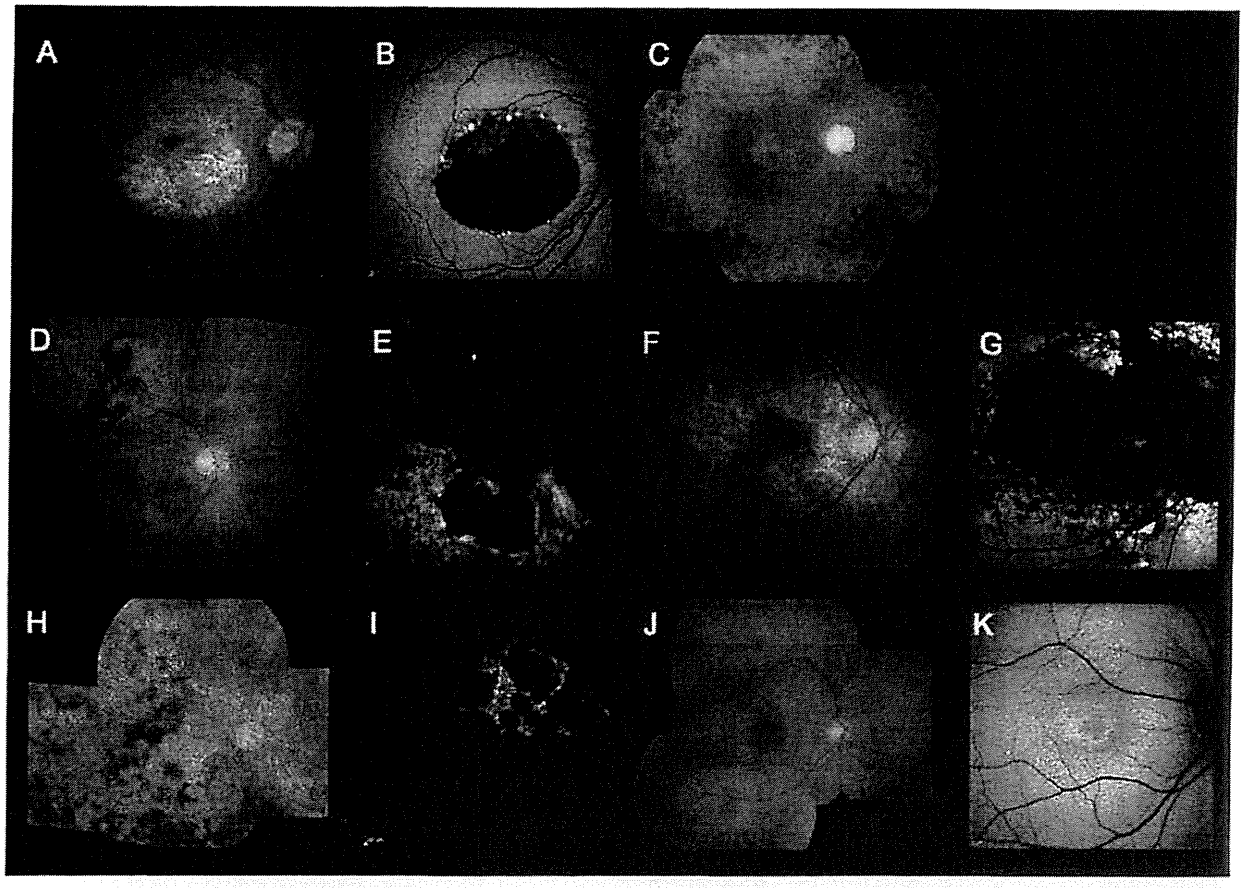

FIGURE 2. Color fundus photographs and autofluorescence images of six cases harboring a single, likely benign, missense variant with "atypical" clinical features for *ABCA4*-associated retinal disease (patients 74, 75, 76, 77, 78, and 79). Color photograph of patient 74 shows a geographic atrophy-like appearance (**A**), which on AF imaging is surrounded by foci of high and low AF signal (**B**). Patient 75 has evidence of generalized retinal atrophy in addition to marked macular atrophy, with dense pigmentation at the level of the RPE, and bone spicule formation, marked vessel attenuation, and optic disc pallor (**C**). Patient 76 has extensive macular atrophy extending beyond the arcades, with dense pigmentation at the level of the RPE and slight bone spicule pigmentation in the periphery (**D**). AF imaging demonstrates a heterogeneous background, but no peripapillary sparing (**E**). Patient 77 has a large area of macular atrophy extending to the optic disc (**F**), which on AF imaging is surrounded by an irregular low AF signal with foci of high and low signal, with no peripapillary sparing (**G**). Patient 78 has multiple widespread areas of atrophy with dense pigmentation at the level of RPE and bone spicule pigmentation in the periphery (**H**). AF imaging identifies multiple low signal areas with a heterogeneous background and no peripapillary sparing (**I**). Patient 79 has subtle atrophy confined to the fovea (**J**). AF imaging demonstrates a localized low AF signal at the fovea surrounded by a homogeneous background (**K**).

disease was calculated as the difference between age at onset and age at the latest examination.

Clinical Assessment

A full medical history was obtained and a comprehensive ophthalmologic examination was performed for all patients. Clinical assessment included best-corrected Snellen visual acuity (converted to equivalent logMAR visual acuity), fundus photography, autofluorescence (AF) imaging, spectral domain optical coherence tomography (SD-OCT), and electrophysiologic assessment.

Color fundus photography was performed with the TRC-50IA Retinal Fundus Camera (Topcon, Tokyo, Japan) and AF images were obtained using either an HRA 2 (excitation wavelength, 488 nm; barrier filter, 500 nm; field of view, 30 × 30°; Heidelberg Engineering, Heidelberg, Germany)[31] or Spectralis with viewing module version 5.1.2.0 (excitation wavelength, 488 nm; barrier filter, 500 nm; fields of view, 30 × 30° and 55 × 55°; Heidelberg Engineering) after pupillary dilation.[32] Patients were classified into one of three AF subtypes based on a recent report in *ABCA4*-associated retinal disease[31]: type 1—localized low AF signal at the fovea surrounded by a homogeneous background, type 2—localized low AF signal at the macula surrounded by a heterogeneous background, and type 3—multiple areas of low AF signal at the posterior pole with a heterogeneous background. SD-OCT imaging was obtained with the Spectralis with viewing module version 5.1.2.0.[32]

Electrophysiologic assessment included full-field electroretinography (ffERG) and pattern electroretinography (PERG) incorporating the standards of the International Society for Clinical Electrophysiology of Vision (ISCEV).[33,34] All components of the ffERG and PERG were taken into account when classifying patients into one of the three electrophysiologic groups:[4,35] group 1—patients with PERG P50 abnormality with normal ERGs, group 2—subjects with PERG P50 abnormality and additional generalized cone ERG abnormality (assessed with light adapted 30 Hz ERG and light adapted 3.0 ERG), and group 3—individuals with PERG P50 abnormality, and addi-